CCT chaperonin complex is required for efficient delivery of anthrax toxin into the cytosol of host cells

Louise H. Slater[a,b,c], Erik C. Hett[a,b,c], Anne E. Clatworthy[a,b,c], Kevin G. Mark[a,b,c], and Deborah T. Hung[a,b,c,1]

[a]Department of Molecular Biology and Center for Computational and Integrative Biology, Massachusetts General Hospital, Boston, MA 02114; [b]Infectious Disease Initiative, Broad Institute, Cambridge, MA 02142; and [c]Department of Microbiology and Immunobiology, Harvard Medical School, Boston, MA 02115

Edited* by R. John Collier, Harvard Medical School, Boston, MA, and approved April 24, 2013 (received for review February 8, 2013)

Bacterial toxins have evolved successful strategies for coopting host proteins to access the cytosol of host cells. Anthrax lethal factor (LF) enters the cytosol through pores in the endosomal membrane formed by anthrax protective antigen. Although in vitro models using planar lipid bilayers have shown that translocation can occur in the absence of cellular factors, recent studies using intact endosomes indicate that host factors are required for translocation in the cellular environment. In this study, we describe a high-throughput shRNA screen to identify host factors required for anthrax lethal toxin-induced cell death. The cytosolic chaperonin complex chaperonin containing t-complex protein 1 (CCT) was identified, and subsequent studies showed that CCT is required for efficient delivery of LF and related fusion proteins into the cytosol. We further show that knockdown of CCT inhibits the acid-induced delivery of LF and the fusion protein LFN-Bla (N terminal domain of LF fused to β-lactamase) across the plasma membrane of intact cells. Together, these results suggest that CCT is required for efficient delivery of enzymatically active toxin to the cytosol and are consistent with a direct role for CCT in translocation of LF through the protective antigen pore.

TCP-1 | TRiC

Anthrax toxin, a bacterial protein toxin produced by *Bacillus anthracis*, is an essential virulence factor that directly causes the pathology associated with anthrax disease. Anthrax toxin is a canonical AB toxin composed of the B subunit protective antigen (PA) and two enzymatic A subunits, lethal factor (LF) and edema factor (EF) (1). LF is a zinc metalloprotease that cleaves MAP kinase kinases (MEKs) and NLRP1 (2, 3), and EF is an adenylate cyclase that converts ATP to cAMP. Individually, the toxin components are not toxic, but a combination of PA and LF (lethal toxin; LT) causes death of mice and rapid caspase-1–dependent cell death of susceptible murine macrophages (4, 5), and a combination of PA and EF (edema toxin; ET) causes edema at the site of injection in experimental animals.

Bacterial toxins have coopted numerous host factors to gain access to the cell and alter host physiology. Cytosolic delivery of anthrax toxin requires binding of PA protein to one of two anthrax toxin receptors (ANTXR1/2) on the surface of host cells, cleavage by a host furin protease, and oligomerization of receptor-associated PA_{63} into heptamers or octamers (1, 6). After binding of LF and/or EF, the toxin–receptor complexes undergo endocytosis and trafficking to endosomes. Upon a decrease in endosomal pH, PA undergoes a conformational change and inserts into the membrane, forming a functional pore through which LF and EF translocate (1).

Unfolding and translocation of the N-terminal domain of LF (LF_N) in vitro occurs in the absence of accessory factors (7). However, we have previously shown that the endosomal chaperone GRP78 (78 kDa glucose regulated protein) facilitates LF_N unfolding in the mildly acidic early endosome (pH 6.5), but not the late endosome (pH 5) (8). Furthermore, translocation of the fusion protein LF_N–DTA (LFN fused to diphtheria toxin fragment A) from endosomes in vitro requires cytosolic factors, including the coatomer protein complex I (COPI) (9). Thus, host factors clearly play an important role in toxin translocation, reflecting remarkable coevolution of a pathogen and the host.

Previous genetic screens have been successful in identification of host factors involved in the LT pathway. A gain-of-function screen that used a cDNA library to complement the defect in PA binding in a toxin-resistant cell line identified ANTXR1 as an anthrax toxin receptor (10). Subsequently, a loss-of-function screen using EST-based gene inactivation identified ARAP3 and low density lipoprotein receptor-related protein 6 (LRP6) as host proteins involved in toxin internalization (11, 12), and a loss-of-function screen using insertional mutagenesis in a haploid human cell line confirmed ANTXR2 as an anthrax toxin receptor (13).

In this study, we have performed a focused, high-throughput RNAi screen to identify host proteins and pathways that are involved in LT-induced cell death. We describe the identification of the chaperonin containing t-complex protein 1 (TCP-1) (CCT)/TCP-1 ring complex, a heterooligomeric complex consisting of eight different subunits (14), as an important host factor for efficient delivery of enzymatically active LF into the host cytosol. Knockdown of CCT inhibits the cellular effects of numerous toxins or toxin fusions including MEK cleavage by LT, cAMP production induced by ET, cell death induced by PA/LF_N-DTA, and β-lactamase activity by PA/LF_N-Bla (LFN genetically fused to β-lactamase (LF_N-Bla). LF-induced cell death and β-lactamase activity were also inhibited in CCT-knockdown cells when LF and LF_N-Bla, respectively, were delivered to the cytosol through PA pores generated directly in the plasma membrane (15), circumventing the requirement for endocytosis and trafficking of the toxin. This finding demonstrates that the likely role of CCT is in the direct translocation of PA pore substrates into the cytosol of host cells.

Results

We set out to identify host proteins and pathways involved in LT-induced cell death by performing an RNAi screen of 1,780 genes from the mouse chaperone, kinase, phosphatase, and vesicle transport families (Table S1) (16). An average of five shRNAs were tested per gene, in arrayed format. After knockdown of the target gene, the cells were challenged with a lytic dose of LT, and cell viability was measured. From the primary screen, ~6.8% (~128 in total) of genes were cherry picked. Because genes that have hits with multiple hairpins are less likely to be caused by off-target effects, we prioritized genes with multiple hairpins that had robust z scores >2 standard deviations from the mean and then cherry picked the remaining genes based on the highest robust z scores and reproducibility between the two replicates

Author contributions: L.H.S., E.C.H., A.E.C., K.G.M., and D.T.H. designed research; L.H.S., E.C.H., A.E.C., and K.G.M. performed research; L.H.S., E.C.H., A.E.C., K.G.M., and D.T.H. analyzed data; and L.H.S., E.C.H., A.E.C., and D.T.H. wrote the paper.

The authors declare no conflict of interest.

*This Direct Submission article had a prearranged editor.

[1]To whom correspondence should be addressed. E-mail: hung@molbio.mgh.harvard.edu.

This article contains supporting information online at www.pnas.org/lookup/suppl/doi:10.1073/pnas.1302257110/-/DCSupplemental.

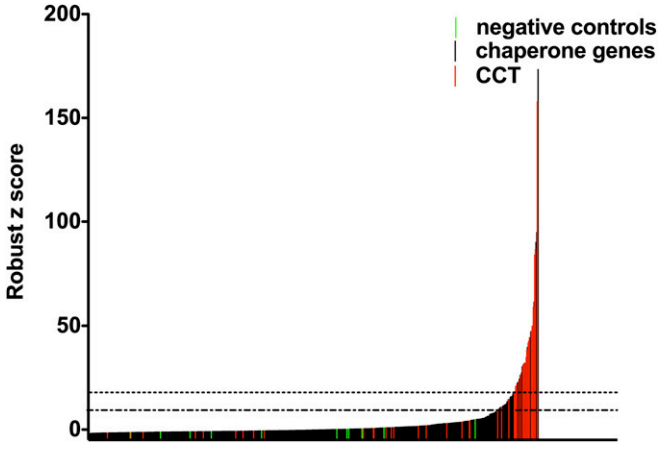

Fig. 1. RNAi screen: primary screening data from the mouse chaperone library. Chaperone genes were knocked down by shRNA, and cells were challenged with LT. The graph shows the mean robust z score for each shRNA tested. shRNAs designed to target nonendogenous genes, such as GFP, are highlighted in green, and shRNAs targeting CCT subunits are highlighted in red. The dotted lines indicate values 1 and 2 SD from the mean.

(Fig. 1). When retested against LT, 80% of cherry-picked genes had at least one protective hairpin. Genes in the top 50% of confirmed hits are shown in Tables S2–S6. Genes from the vesicle trafficking library comprised a significant proportion of the top hits. This finding is unsurprising given the requirement for endocytosis and vesicle trafficking in cytoplasmic delivery of LT. Among the confirmed hits were several host factors known to be involved in LT-induced cell death, including caspase-1, Bnip3, dynamin, vacuolar H^+-ATPase (v-ATPase), GRP78, and members of the COPI coatamer complex.

By far the most striking hits from the RNAi screen were genes encoding the cytosolic chaperonin CCT complex (Fig. 1 and Tables S3 and S7). Eight of nine genes encoding CCT subunits were hits, with multiple protective shRNAs per subunit (Table S7). These shRNAs were among the strongest hits in the screen and afforded a greater degree of protection than caspase-1, v-ATPase, GRP78, and the COPI complex. Surprisingly, CCT6-1 and -2 were both hits, whereas shRNAs targeting CCT1, which is thought to be an essential CCT subunit (17), did not afford protection. CCT6-1 and -2 share 81% amino acid sequence identity, compared with ~30% identity between other CCT subunits, and are thought to be alternative subunits (18). CCT6-1 is widely expressed and is thought to be the predominant CCT6 subunit, whereas CCT6-2 mRNA has only been detected in mouse testis. However, in this study, both CCT6-1 and -2 mRNA were detected in J774A.1 cells lysates by RT-PCR (Fig. S1), raising the possibility that CCT6-1 and -2, but not CCT1, are components of a noncanonical CCT chaperonin complex in J774A.1 cells.

The strong phenotype, coupled with the large number of active shRNAs, suggested that CCT plays an important role in the LT pathway. We retested the susceptibility of J774A.1 cells to LT over a range of LF concentrations and found that up to 49% of CCT-knockdown cells were still viable after LT treatment, compared with 3% for a nontargeting shRNA (Fig. 2 *A* and *B*). Lysates from CCT-knockdown cells were probed by immunoblot to confirm knockdown of the target protein (Fig. 2*C*).

Because the RNAi screen had the potential to identify important host factors at all stages of the LT pathway, we tested whether CCT knockdown affected cytosolic delivery of LF or a step downstream of enzymatic activity. To distinguish between these two possibilities, we tested the ability of CCT knockdown to inhibit intoxication by the related A subunits EF and LF_N-DTA, which also traffick to the cytosol in a PA-dependent manner identical to LT, but have different enzymatic activities. LF_N-DTA consists of the N-terminal domain of LF genetically fused to the enzymatic domain of diphtheria toxin and induces apoptosis by ADP ribosylation of elongation factor 2 and inhibition of protein synthesis (19), in contrast to the rapid caspase-1–dependent cell death induced by LF (5). Knockdown of CCT prevented the increase in cAMP stimulated by ET and cell death induced by a combination of PA and LF_N-DTA (Fig. 3 *A*–*C*). Furthermore, knockdown of CCT inhibited MEK cleavage upon LT treatment (Fig. 3*D*). Thus, the ability of CCT knockdown to prevent intoxication by LT, ET, and PA/LF_N-DTA suggests that CCT is involved in a common step upstream of toxin cytosolic activity.

CCT is an important cellular chaperonin, particularly in the biogenesis of actin and tubulin, and therefore has an indirect role in various cellular pathways. Knockdown of CCT has been reported to cause a block in cell-cycle progression, disordered cytoskeleton, and a reduction in cell motility (20). Therefore, we wondered whether CCT knockdown could affect receptor recycling and whether resistance to LT could be a result of a reduction in cell surface anthrax toxin receptor levels. Although J774A.1 cells have been reported to express both ANTXR1 and ANTXR2 (21), we found that ANTXR2 was the principal, if not sole, mediator of LT-induced cell death. siRNA knockdown of ANTXR2, or blocking of ANTXR2 receptors with an anti-ANTXR2 antibody, afforded 100% protection against LT, whereas knockdown of ANTXR1 did not alter cell viability (Fig. S2 *A* and *B*). Thus, to test whether ANTXR2 levels are altered in CCT-knockdown cells, we performed flow cytometry analysis using an anti-ANTXR2 antibody. We detected a small decrease

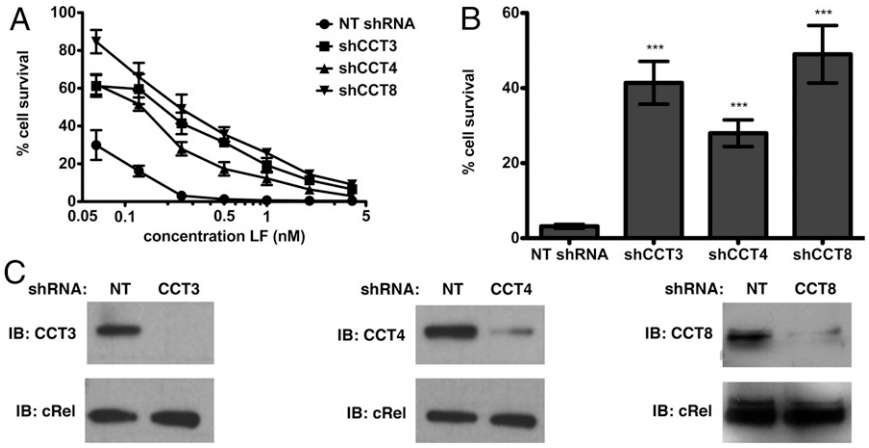

Fig. 2. Knockdown of CCT subunits in J774A.1 cells confers resistance to LT. CCT knockdown in J774A.1 cells was allowed to proceed for 5 d. (*A* and *B*) Cell survival after challenge with PA (11 nM) and LF for 6 h at 37 °C. *B* shows cell survival at 0.25 nM LF. NT, nontargeting shRNA. Data are expressed as mean ± SD of three technical replicates. ***$P < 0.001$ (*C*) Western blot to indicate the extent of CCT knockdown. cRel was used as a loading control.

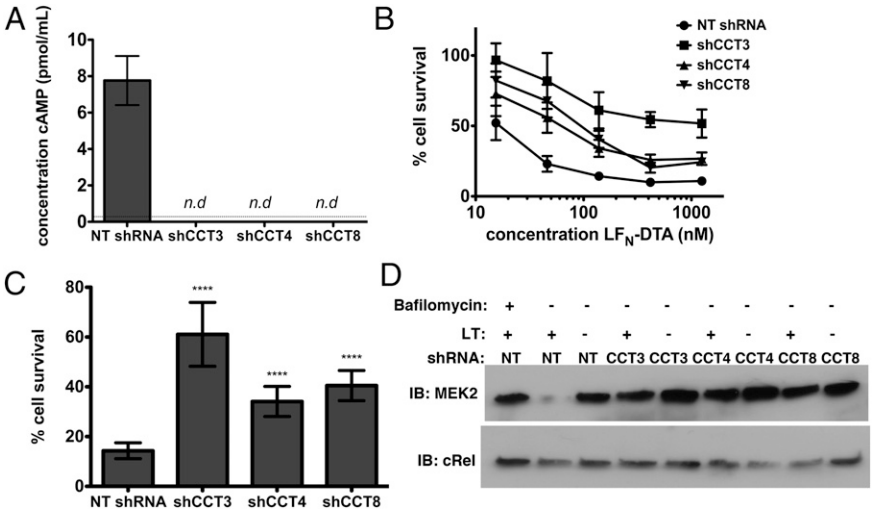

Fig. 3. CCT is involved in a step upstream of toxin cytosolic activity. CCT knockdown in J774A.1 cells was allowed to proceed for 7 d. (*A*) cAMP concentration after treatment with PA and EF. The dotted line indicates the limit of detection; cAMP was not detected in shCCT cells. n.d, not detected. Data are expressed as mean ± SD of two technical replicates. (*B* and *C*) Cell survival after challenge with PA (18 nM) and LF_N-DTA. The column graph in *C* shows cell survival at 139 pM LF_N-DTA. Data are expressed as mean ± SD of eight technical replicates. ****$P < 0.0001$. (*D*) Western blot to demonstrate MEK cleavage after cells were challenged with LF and PA. cRel was used as a loading control.

in cell surface ANTXR2, suggesting that CCT can affect, to a small degree, receptor biogenesis or recycling (Fig. S2 *C–E*).

To test whether this modest reduction of cell-surface ANTXR2 was sufficient to account for the robust resistance to LT observed with CCT knockdown, we looked to see whether amounts of LT sufficient to kill host cells were still able to reach the endosome in CCT-knockdown cells. To measure the amount of LT in the endosome, we took advantage of the fact that the PA pore that forms in the endosome is SDS-resistant. We noted that in CCT4 knockdown cells, there was no inhibition of PA pore formation, demonstrating that CCT is required only after the toxin reaches the endosome. We did observe partial inhibition of PA pore formation in CCT3 and CCT8 knockdown cells. To test whether this small amount of inhibition of pore formation is sufficient to account for the observed protection against cell death, we constructed a standard curve by titrating different amounts of PA and LF in cells (using cells expressing nontargeting shRNA) and correlating the amount of PA pore formation in the endosome with the amount of cell death (Fig. 4 *A* and *B*). We found that the amount of PA, and thus LF, that is able to get into the endosome in CCT3 and CCT8 knockdown cells should be sufficient to kill J774.1 cells if LF were able to pass from the endosome to the cytosol (Fig. 4 *A–C*). Thus, CCT is playing a role in toxin delivery that is not accounted for by the slight reduction in ANTXR2 that is observed with CCT knockdown.

To further confirm that CCT plays a role in the translocation step, we tested whether CCT was required for LT-induced cell death when LF was delivered through PA pores formed directly in the plasma membrane, thus bypassing the need for endocytosis of toxin–receptor complexes and trafficking to the endosome (15). PA and LF were bound to the surface of J774A.1 cells at 4 °C, and PA pore formation and LF translocation at the cell surface were induced by incubation in pH 5 buffer at 37 °C for 2 min. Cells were washed to remove excess free, unbound toxin, incubated in complete medium containing the v-ATPase inhibitor bafilomycin A1 to inhibit entry of any residual toxin via the endocytic route, and cell viability was measured after 6 h (Fig. 5*A*). We found that knockdown of CCT strongly inhibited cell death induced by LT in this system (Fig. 5*B*). Furthermore, CCT knockdown did not alter the amount of SDS-resistant PA pore at the cell surface at all, confirming that a reduction in ANTXR2 does not account for the increased resistance to LT in this system (Fig. 5*C*). Together with our data showing that CCT knockdown inhibits a step upstream of LF cytosolic activity, this result focusing on toxin delivery at the cell surface further supports the hypothesis that CCT has a direct role in translocation

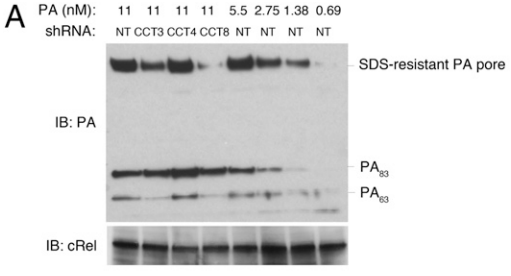

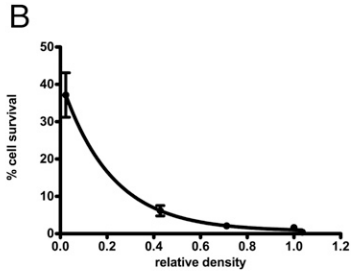

C

shRNA	Relative density PA pore at 11 nM	Expected cell survival at 0.5 nM LF (%)	Actual cell survival at 11 nM PA, 0.5 nM LF (%)	Actual cell survival at 11 nM PA, 2 nM LF (%)
CCT3	0.66	2.5	43	22
CCT4	1.03	0.98	37	23
CCT8	0.17	19.0	80	44
NT shRNA	1.00	1.04	1.65	1.32

Fig. 4. Lethal levels of anthrax toxin reach endosomes in CCT-knockdown cells. Knockdown of CCT in J774A.1 cells was allowed to proceed for 5 d. (*A*) Western blot to demonstrate PA pore formation after incubation with PA for 30 min. cRel was used as a loading control. (*B*) Standard curve showing extent of PA pore formation in nontargeting shRNA-expressing cells treated with various concentrations of PA as deduced by Western blot quantification and the corresponding amount of cell survival in cells treated with the same concentrations of PA and 0.5 nM LF for 6 h at 37 °C. (*C*) Table showing the expected amount of cell survival at 0.5 nM LF as predicted by the standard curve in *B*, and the actual amount of cell survival observed when cells were treated with 11 nM PA and the indicated concentration of LF.

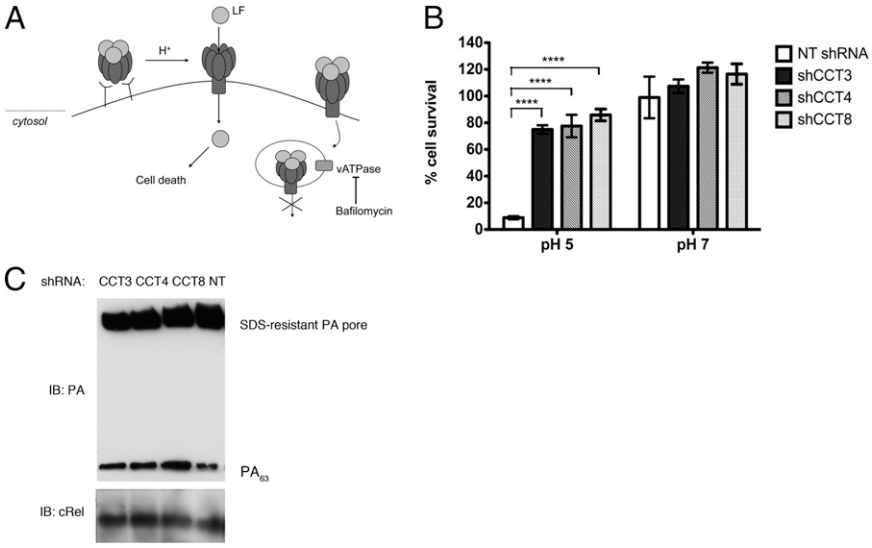

Fig. 5. CCT knockdown inhibits cell death induced by LF delivered through PA pores in the plasma membrane. (*A*) Schematic of the assay. (*B*) Knockdown of CCT in J774A.1 cells was allowed to proceed for 5 d. Graph shows cell survival after LF was delivered through PA pores in the cell membrane. Cells were incubated sequentially with PA and LF at 4 °C, and PA pore formation and translocation were initiated by incubation with pH 5 translocation buffer for 2 min at 37 °C. After translocation, cells were incubated for 4 h at 37 °C in complete medium with 100 nM bafilomycin A1, and cell viability was measured. Incubation at pH 7 does not induce PA pore formation or LF translocation. Data are expressed as mean ± SD of three technical replicates. ****$P < 0.0001$. (*C*) Immediately after translocation at pH 5, cells were washed, lysed, and subjected to SDS/PAGE, followed by immunoblot using an anti-PA antibody. cRel was used as a loading control.

or refolding of LF. Because CCT is a cytosolic chaperonin, we hypothesize that it might interact with the nascent polypeptide chain of LF as it emerges through the PA pore, in a manner similar to the way in which it interacts with its native substrates as they are synthesized by the ribosome (22).

To investigate whether CCT could be acting during translocation or refolding of LF, we created another fusion protein, LF_N-Bla. β-Lactamase is known to fold in the absence of accessory factors (23), therefore allowing us to dissect the role of CCT in translocation alone. After incubation with PA and LF_N-Bla, β-lactamase activity could be detected in the cytosol of J774A.1 cells, and this activity was inhibited by CCT knockdown (Fig. 6*A*). CCT knockdown also inhibited β-lactamase activity when LF_N-Bla was delivered to the cytosol by translocation through PA pores at the plasma membrane (Fig. 6*B*). Thus, using the cell surface translocation assay described above, we have shown that CCT is required for β-lactamase cytosolic accumulation, indicating that CCT likely facilitates translocation of toxins with the LF_N through the PA pore.

Discussion

Bacterial protein toxins have evolved sophisticated methods to gain access to the cytosol of host cells and alter host physiology. Anthrax toxin presents a convenient system for studying toxin translocation. Unfolding and translocation of LF_N, in vitro, is achieved by acidic pH along with interaction of the unfolding polypeptide with the hydrophobic α and ϕ clamps of the PA pore (24, 25) and occurs in the absence of accessory factors (7). Translocation through PA pores formed in the artificial bilayer system proceeds by means of a charge-state–dependent Brownian ratchet mechanism that requires a pH gradient across the membrane (25).

However, unfolding and translocation in the crowded environment of the cell may pose additional challenges to the unfolded polypeptide, such as aggregation, and therefore accessory factors may be required to increase the efficiency of toxin delivery. We have previously shown that LF_N unfolding in the early endosome (pH 6.5), but not the late endosome (pH 5), is facilitated by the endosomal chaperone GRP78 (8). Furthermore, translocation of LF_N-DTA from isolated endosomes requires the COPI coatamer complex, in addition to other, previously unidentified, cytoplasmic factors (9). The related AB toxins diphtheria and *Clostridium botulinum* C2 toxin share a requirement with LT for the COPI complex; however, unlike LT, diphtheria, *C. botulinum* C2 toxin, *Clostridium difficile* transferase, and *Clostridium perfringens* iota-toxin also require heat shock protein 90 (Hsp90) and cyclophilin A (26–30).

In this study, we have conducted a high-throughput RNAi screen to identify host proteins and pathways required for LT-induced cell death. We identified the cytoplasmic chaperonin CCT and show that it is required for LT-induced cell death. We identified multiple shRNAs targeting eight of nine CCT subunits that are protective against LT. Knockdown of CCT also inhibited MEK cleavage by LT as well as intoxication by ET and PA/LF_N-DTA, suggesting that its role is in toxin entry, upstream of toxin cytosolic activity. Furthermore, we show that CCT knockdown inhibits cell death and β-lactamase activity induced when LF and LF_N-Bla, respectively, are delivered through PA pores in the plasma membrane. Because this route of entry circumvents the requirements for endocytosis and toxin trafficking, and because β-lactamase is known to fold in the absence of accessory factors (23), this finding suggests that the role of CCT in toxin delivery is likely in translocation through the PA pore.

Although CCT could facilitate toxin translocation or refolding in an indirect manner, its role as a cellular chaperone suggests that it could directly interact with the unfolded polypeptide chain as it emerges through the PA pore, in analogy to the nascent

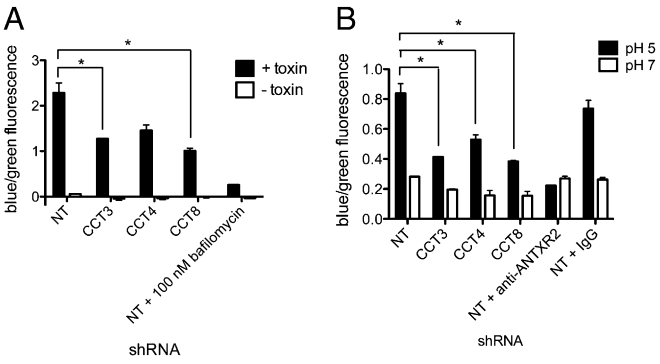

Fig. 6. CCT knockdown inhibits translocation of LF_N-Bla to the cytosol of host cells. (*A*) β-Lactamase activity after J774A.1 cells were incubated with PA and LF_N-Bla at 37 °C. β-Lactamase activity was measured by FRET using the substrate CCF2AM. Uncleaved substrate emits green fluorescence, and cleaved substrate emits blue fluorescence. (*B*) β-Lactamase activity after LF_N-Bla was delivered to the cytosol through PA pores in the cell membrane. Data are expressed as mean ± SD of two technical replicates. *$P < 0.05$.

polypeptide forming at the ribosome. To do so, CCT must be targeted to endosomes. Because CCT substrates are delivered by upstream chaperones, such as Hsp70 and prefoldin (31, 32), CCT may be recruited to endosomes by upstream chaperones that recognize the nascent, unfolded LF chain as it emerges from the PA pore.

The current model for anthrax toxin translocation suggests that LF and EF are translocated into the lumen of intraluminal vesicles, and delivered to the cytosol when the vesicles undergo back fusion with the limiting membrane of the late endosome (33). Intraluminal vesicles are formed from invagination and fission of early endosomal membrane and therefore contain cytosol (34). Thus, the participation of cellular factors such as CCT and the COPI complex in translocation is not inconsistent with this model.

In vivo, CCT folds a discrete set of endogenous substrates, including its primary substrates actin and tubulin, along with a number of cell-cycle control proteins and several proteins containing WD β-propellor domains (17, 35). There is evidence to suggest that at least some CCT substrates bind in a partly structured form and use specific binding determinants to contact particular CCT subunits (36–38); however, there is no specific sequence or structural motif shared by all CCT substrates. The substrate binding sites on CCT contain different combinations of hydrophobic and polar residues and therefore present various binding surfaces for substrates (38). Just as CCT interacts with a discreet subset of cellular proteins, this study suggests that it can also interact with nonendogenous proteins. In fact, an analysis of the CCT interactome revealed that CCT interacts with several exogenous proteins, including the Epstein–Barr virus nuclear antigen, hepatitis B virus capsid protein, and p4 of Mason–Pfizer monkey virus (39). Further, NS5B, the hepatitis C RNA-dependent RNA polymerase (40), and PB2 of the influenza A RNA polymerase (41) also interact with CCT, and knockdown of CCT inhibits viral replication. This finding suggests that, despite the selectivity CCT appears to display for its endogenous substrates, certain pathogens have evolved to coopt CCT to promote their own life cycle.

The identification of CCT as a cellular chaperone required for cytoplasmic delivery of anthrax toxin highlights the differences between toxin translocation in vitro and in vivo and underscores the emerging role of host factors required in in vivo systems. A model is thus emerging that demonstrates the number of host proteins that are recruited by the toxin to facilitate its delivery and, ultimately, its induction of cell death.

Materials and Methods

Cells, Antibodies, and Reagents. J774A.1 cells were obtained from American Type Cell Culture Collection. Rabbit polyclonal IgG antibody to CCT3 (H-300), mouse monoclonal IgG_1 antibody to CCT4 (H-1), rabbit polyclonal IgG antibody to the N terminus of MEK2, rabbit polyclonal IgG antibody to reticuloendotheliosis oncogene (cRel), secondary HRP goat anti-rabbit antibody, secondary HRP goat anti-mouse antibody, and secondary HRP goat anti-rat antibody were from Santa Cruz Biotechnology. Rat monoclonal IgG_{2a} antibody to CCT8 (PK/13/72/8k) was from AbD Serotec. Goat polyclonal IgG antibody to ANTXR2 was from R&D Systems. Rabbit polyclonal IgG antibody to PA was a gift from the Collier Laboratory (Harvard Medical School). Alexa Fluor 488 donkey anti-goat IgG antibody was from Invitrogen.

Protein Expression and Purification. PA and LF were expressed in BL21STAR (DE3) *Escherichia coli* grown in ECPM1 medium. Cultures were induced at 30 °C with isopropyl-1-thio-β-D-galactopyranoside. Recombinant PA was overexpressed in the periplasm from pET22b (Invitrogen) and purified as described (42). His_6-tagged LF and LF_N-Bla cloned into pET15b were purified as described (43).

RNAi Screen. A total of 1×10^3 J774A.1 cells per well in white, optical 384-well plates were infected with 5 μL of lentivirus in medium containing 8 μg/mL polybrene by centrifugation at $350 \times g$ for 90 min at 32 °C. Following infection, the supernatant was replaced with 30 μL of medium. At 24 and 96 h after infection, 2.5 μg/mL puromycin was used to select for stable transductants. Seven days after infection, cells were incubated with 11 nM PA and 2 nM LF in fresh medium for 6 h at 37 °C. An equal volume of Cell Titer Glo (Promega), diluted to a ratio of 1:6 in PBS, was added to each well, and luminescence was measured by using an Envision Multilabel Plate Reader (Perkin-Elmer). For follow-up studies, lentiviral infection was scaled up to 96- or 6-well plates. The nontargeting shRNA clonetechGFP_49s1c1 (TRCN0000072201; GTCGAGCTGGACGGCGACGTA) was used as a negative control.

Lentivirus Production. For follow-up studies, lentivirus was produced in 293T cells by transient transfection. Transfection mixes contained 1 μg of the pLKO.1 vector plasmid, 100 ng of the pCMV-VSV-G envelope plasmid, 900 ng of the psPAX2 packaging plasmid, and 6 μL of Fugene-6 (Roche) and were made up according to the manufacturer's instructions in 200 μL of Opti-MEM-1 (minimal essential medium) (Gibco). Transfection mixes were added to 3×10^5 293T cells in six-well plates in antibiotic-free medium and incubated overnight. Twenty-four hours later, medium was replaced with 2 mL of viral harvest medium [DMEM with 30% (vol/vol) FBS]. Viral supernatants were collected at 48 and 72 h posttransfection.

Western Blots. J774A.1 cells in six-well plates were washed three times with PBS and lysed in radioimmunoprecipitation assay buffer (50 mM Hepes–NaOH, pH 7.4, 1% Nonidet P-40, 150 mM sodium chloride, 4 mM EDTA) containing Complete Mini protease inhibitor mixture (Roche). Lysate was separated by SDS/PAGE and transferred to PVDF, followed by immunoblot with primary and HRP-conjugated secondary antibody. Blots were visualized by using SuperSignal West Femto or Pico substrate (Pierce).

MEK Cleavage Assay. CCT knockdown cells were incubated with PA (11 nM) and LF (0.125 nM) for 2.5 h at 37 °C. Western blots were performed with anti-MEK2 and cRel antibodies.

ET Assays. EF was obtained from List Biological Laboratories. J774A.1 cells in 384-well plates were incubated with 11 nM PA and 3.7 nM EF for 5 h at 37 °C, and the concentration of cAMP was measured by cAMP enzyme immunoassay according to the manufacturers instructions (Enzo Life Sciences).

LF_N-DTA Assays. J774A.1 cells in 384-well plates were incubated with PA (18 nM) and the indicated concentration of LF_N-DTA for 30 h at 37 °C. Cell viability was measured with Cell Titer Glo as described.

Antibody Inhibition of ANTXR2. J774A.1 cells were incubated for 1 h at 4 °C with cold DMEM containing 1% FBS and 38 μg/mL goat anti-ANTXR2 antibody, before addition of LT.

PA Pore Formation Assay and Quantification of Western Blots. J774A.1 cells were incubated with the indicated concentration of PA for 30 min at 37 °C. Western blots were carried out with rabbit IgG anti-PA antibody and secondary HRP goat anti-rabbit antibody. For quantification, blots were scanned by using an Epson Perfection V700 photo flatbed scanner and analyzed by using ImageJ software (44).

Acid-Induced Delivery of LF Through PA Pores Formed in the Plasma Membrane. J774A.1 cells were incubated with 3.5 μg/mL PA_{63} in OPTI-MEM-1 for 2 h at 4 °C. Cells were washed once with cold PBS and incubated with 3.5 μg/mL LF in OPTI-MEM-1 for 2 h at 4 °C. Cells were washed twice and incubated with 100 μL of translocation buffer (20 mM MES, 150 mM sodium chloride, 5 mM gluconic acid) at pH 5 for 2 min at 37 °C. Cells were washed three times and incubated for 4 h at 37 °C in complete medium with 100 nM bafilomycin A1, and cell viability was measured by using Cell Titer Glo as described. Cells were washed and lysed directly after translocation for Western blots.

β-Lactamase Assay. For delivery of toxin through the endocytic route, cells were pretreated with 100 nM bafilomycin for 1 h at 37 °C and then incubated with 6.4 nM PA and LF_N-Bla for 1 h at 37 °C. For translocation of toxin across the plasma membrane, control wells were pretreated with 40 μg/mL ANTXR2 antibody or goat IgG, and then the translocation assay protocol was followed with 30 μg/mL PA_{63} and LF_N-Bla. Cells were washed with HBSS, and β-lactamase activity was measured by using the In Vivo Gene Blazer FRET assay (Invitrogen). After incubation with CCF2AM substrate in HBSS for 1 h at room temperature, cells were washed once with HBSS and incubated in HBSS for 30–45 min at room temperature before fluorescence was measured

by using a plate reader. All washing and incubation steps after incubation with toxin included 100 nM bafilomycin.

Statistical Analysis. Data are expressed as mean ± SD. Significance of differences between groups was determined by Student *t* test. Values of $P < 0.05$ were taken as statistically significant.

ACKNOWLEDGMENTS. We thank A. Barker and A. McCluskey for help with production and purification of PA, LF, and LF_N-Bla; and the Broad Institute RNAi screening platform for technical help. E.C.H. was supported by National Institutes of Health (NIH) National Research Service Award Fellowship F32AI084323. This work was supported, in part, by NIH Grant U54 AI057159 to the New England Center of Excellence/Biodefense and Emerging Infectious Diseases (D.T.H.).

1. Collier RJ (2009) Membrane translocation by anthrax toxin. *Mol Aspects Med* 30(6): 413–422.
2. Levinsohn JL, et al. (2012) Anthrax lethal factor cleavage of Nlrp1 is required for activation of the inflammasome. *PLoS Pathog* 8(3):e1002638.
3. Duesbery NS, et al. (1998) Proteolytic inactivation of MAP-kinase-kinase by anthrax lethal factor. *Science* 280(5364):734–737.
4. Boyden ED, Dietrich WF (2006) Nalp1b controls mouse macrophage susceptibility to anthrax lethal toxin. *Nat Genet* 38(2):240–244.
5. Fink SL, Bergsbaken T, Cookson BT (2008) Anthrax lethal toxin and Salmonella elicit the common cell death pathway of caspase-1-dependent pyroptosis via distinct mechanisms. *Proc Natl Acad Sci USA* 105(11):4312–4317.
6. van der Goot G, Young JA (2009) Receptors of anthrax toxin and cell entry. *Mol Aspects Med* 30(6):406–412.
7. Krantz BA, Finkelstein A, Collier RJ (2006) Protein translocation through the anthrax toxin transmembrane pore is driven by a proton gradient. *J Mol Biol* 355(5):968–979.
8. Tamayo AG, et al. (2011) GRP78(BiP) facilitates the cytosolic delivery of anthrax lethal factor (LF) in vivo and functions as an unfoldase in vitro. *Mol Microbiol* 81(5): 1390–1401.
9. Tamayo AG, Bharti A, Trujillo C, Harrison R, Murphy JR (2008) COPI coatomer complex proteins facilitate the translocation of anthrax lethal factor across vesicular membranes in vitro. *Proc Natl Acad Sci USA* 105(13):5254–5259.
10. Bradley KA, Mogridge J, Mourez M, Collier RJ, Young JA (2001) Identification of the cellular receptor for anthrax toxin. *Nature* 414(6860):225–229.
11. Lu Q, Wei W, Kowalski PE, Chang AC, Cohen SN (2004) EST-based genome-wide gene inactivation identifies ARAP3 as a host protein affecting cellular susceptibility to anthrax toxin. *Proc Natl Acad Sci USA* 101(49):17246–17251.
12. Wei W, Lu Q, Chaudry GJ, Leppla SH, Cohen SN (2006) The LDL receptor-related protein LRP6 mediates internalization and lethality of anthrax toxin. *Cell* 124(6): 1141–1154.
13. Carette JE, et al. (2009) Haploid genetic screens in human cells identify host factors used by pathogens. *Science* 326(5957):1231–1235.
14. Horwich AL, Fenton WA, Chapman E, Farr GW (2007) Two families of chaperonin: physiology and mechanism. *Annu Rev Cell Dev Biol* 23:115–145.
15. Wesche J, Elliott JL, Falnes PO, Olsnes S, Collier RJ (1998) Characterization of membrane translocation by anthrax protective antigen. *Biochemistry* 37(45):15737–15746.
16. Moffat J, et al. (2006) A lentiviral RNAi library for human and mouse genes applied to an arrayed viral high-content screen. *Cell* 124(6):1283–1298.
17. Sternlicht H, et al. (1993) The t-complex polypeptide 1 complex is a chaperonin for tubulin and actin in vivo. *Proc Natl Acad Sci USA* 90(20):9422–9426.
18. Kubota H, Hynes GM, Kerr SM, Willison KR (1997) Tissue-specific subunit of the mouse cytosolic chaperonin-containing TCP-1. *FEBS Lett* 402(1):53–56.
19. Kochi SK, Collier RJ (1993) DNA fragmentation and cytolysis in U937 cells treated with diphtheria toxin or other inhibitors of protein synthesis. *Exp Cell Res* 208(1):296–302.
20. Grantham J, Brackley KI, Willison KR (2006) Substantial CCT activity is required for cell cycle progression and cytoskeletal organization in mammalian cells. *Exp Cell Res* 312(12):2309–2324.
21. Maldonado-Arocho FJ, Fulcher JA, Lee B, Bradley KA (2006) Anthrax oedema toxin induces anthrax toxin receptor expression in monocyte-derived cells. *Mol Microbiol* 61(2):324–337.
22. Frydman J, Nimmesgern E, Ohtsuka K, Hartl FU (1994) Folding of nascent polypeptide chains in a high molecular mass assembly with molecular chaperones. *Nature* 370(6485):111–117.
23. Walker KW, Gilbert HF (1994) Effect of redox environment on the in vitro and in vivo folding of RTEM-1 beta-lactamase and Escherichia coli alkaline phosphatase. *J Biol Chem* 269(45):28487–28493.
24. Feld GK, et al. (2010) Structural basis for the unfolding of anthrax lethal factor by protective antigen oligomers. *Nat Struct Mol Biol* 17(11):1383–1390.
25. Krantz BA, et al. (2005) A phenylalanine clamp catalyzes protein translocation through the anthrax toxin pore. *Science* 309(5735):777–781.
26. Dmochewitz L, et al. (2011) Role of CypA and Hsp90 in membrane translocation mediated by anthrax protective antigen. *Cell Microbiol* 13(3):359–373.
27. Haug G, et al. (2003) The host cell chaperone Hsp90 is essential for translocation of the binary Clostridium botulinum C2 toxin into the cytosol. *J Biol Chem* 278(34): 32266–32274.
28. Kaiser E, et al. (2011) Membrane translocation of binary actin-ADP-ribosylating toxins from Clostridium difficile and Clostridium perfringens is facilitated by cyclophilin A and Hsp90. *Infect Immun* 79(10):3913–3921.
29. Kaiser E, Pust S, Kroll C, Barth H (2009) Cyclophilin A facilitates translocation of the Clostridium botulinum C2 toxin across membranes of acidified endosomes into the cytosol of mammalian cells. *Cell Microbiol* 11(5):780–795.
30. Ratts R, et al. (2003) The cytosolic entry of diphtheria toxin catalytic domain requires a host cell cytosolic translocation factor complex. *J Cell Biol* 160(7):1139–1150.
31. Cuéllar J, et al. (2008) The structure of CCT-Hsc70 NBD suggests a mechanism for Hsp70 delivery of substrates to the chaperonin. *Nat Struct Mol Biol* 15(8):858–864.
32. Vainberg IE, et al. (1998) Prefoldin, a chaperone that delivers unfolded proteins to cytosolic chaperonin. *Cell* 93(5):863–873.
33. Abrami L, Lindsay M, Parton RG, Leppla SH, van der Goot FG (2004) Membrane insertion of anthrax protective antigen and cytoplasmic delivery of lethal factor occur at different stages of the endocytic pathway. *J Cell Biol* 166(5):645–651.
34. Gruenberg J, Stenmark H (2004) The biogenesis of multivesicular endosomes. *Nat Rev Mol Cell Biol* 5(4):317–323.
35. Dekker C, et al. (2008) The interaction network of the chaperonin CCT. *EMBO J* 27(13): 1827–1839.
36. Llorca O, et al. (2000) Eukaryotic chaperonin CCT stabilizes actin and tubulin folding intermediates in open quasi-native conformations. *EMBO J* 19(22):5971–5979.
37. McCormack EA, Rohman MJ, Willison KR (2001) Mutational screen identifies critical amino acid residues of beta-actin mediating interaction between its folding intermediates and eukaryotic cytosolic chaperonin CCT. *J Struct Biol* 135(2):185–197.
38. Spiess C, Miller EJ, McClellan AJ, Frydman J (2006) Identification of the TRiC/CCT substrate binding sites uncovers the function of subunit diversity in eukaryotic chaperonins. *Mol Cell* 24(1):25–37.
39. Yam AY, et al. (2008) Defining the TRiC/CCT interactome links chaperonin function to stabilization of newly made proteins with complex topologies. *Nat Struct Mol Biol* 15(12):1255–1262.
40. Inoue Y, et al. (2011) Chaperonin TRiC/CCT participates in replication of hepatitis C virus genome via interaction with the viral NS5B protein. *Virology* 410(1):38–47.
41. Fislová T, Thomas B, Graef KM, Fodor E (2010) Association of the influenza virus RNA polymerase subunit PB2 with the host chaperonin CCT. *J Virol* 84(17):8691–8699.
42. Wigelsworth DJ, et al. (2004) Binding stoichiometry and kinetics of the interaction of a human anthrax toxin receptor, CMG2, with protective antigen. *J Biol Chem* 279(22): 23349–23356.
43. Zhang S, Finkelstein A, Collier RJ (2004) Evidence that translocation of anthrax toxin's lethal factor is initiated by entry of its N terminus into the protective antigen channel. *Proc Natl Acad Sci USA* 101(48):16756–16761.
44. Abramoff MD, Magalhaes PJ, Ram SJ (2004) Image processing with ImageJ. *Biophotonics International* 11(7):36–42.